

Molecular Phenotype of Spontaneously Arising 4N (G_2 -Tetraploid) Intermediates of Neoplastic Progression in Barrett's Esophagus¹

Michael T. Barrett,² David Pritchard, Corinna Palanca-Wessels, Judy Anderson, Brian J. Reid, and Peter S. Rabinovitch³

Divisions of Human Biology [M. T. B., B. J. R., P. S. R.] and Public Health Sciences [B. J. R.], Fred Hutchinson Cancer Research Center, Seattle, Washington 98104; LifeSpan Biosciences, Seattle, Washington 98121 [D. P.]; and Departments of Medicine (Gastroenterology Division) [B. J. R.], Pathology [C. P.-W., J. A., P. S. R.], and Genetics [B. J. R.], University of Washington, Seattle, Washington 98195

ABSTRACT

Elevated 4N (G_2 -tetraploid) cell populations are unstable intermediates in the development of many human cancers. However, 4N cell populations are intermixed with larger diploid fractions *in vivo*, limiting investigation of these key intermediates of neoplastic progression. Therefore, to study elevated 4N cell populations in human neoplasia, we used flow cytometry to purify populations of spontaneously arising $TP53^{wt}$ and $TP53^{mut}$ 4N cells from cell strains derived from premalignant Barrett's esophagus biopsies. Using oligonucleotide arrays, we identified 625 genes differentially expressed in at least one replicate 2N/4N comparison in each strain and in *hTERT*-immortalized cultures of the $TP53^{mut}$ strains. Strikingly, when hierarchically clustered, these data contained a large node of 124 genes that were up-regulated in 4N $TP53^{mut}$ cells in the absence of condensed chromosomes. Most of these genes function in G_2 -M to mediate processes such as chromosome condensation and segregation. These results describe the molecular phenotype of dysregulated G_2 -M functions and cell cycle checkpoints in a key intermediate of human neoplastic progression.

INTRODUCTION

Neoplastic progression frequently arises as a result of an acquired genetic instability and the subsequent evolution of clonal populations with accumulated genetic lesions. This nonlinear evolutionary process typically involves the appearance of multiple cell lineages with combinations of somatic lesions. One of the most common lesions in human cancers is the development of ploidy abnormalities. Elevated 4N (G_2 -tetraploid) cell populations have been detected in several human neoplasias and are associated with subsequent progression in a variety of cancers (1, 2). We have shown that in patients with the premalignant condition BE,⁴ increased 4N flow-cytometric fractions ($\geq 6\%$) arise interdependently with $TP53$ lesions in diploid cells, predict progression to aneuploidy, and have a 57% chance of progressing to cancer within 5 years (3–7). However, 4N cell populations are transient intermediates and intermixed with larger diploid fractions *in vivo*, limiting investigation of these key intermediates of neoplastic progression. Studies in model systems have shown that elevated 4N fractions and the development of aneuploidy are associated with loss of cell cycle regulation, including lesions in the $TP53$ and Rb pathways, inactivation of G_2 -M checkpoints, and disruption of the mitotic spindle (8–12). However, these studies have relied primarily on immortalized cell systems and cell cycle synchronization, which is often difficult to maintain, in order to purify 4N cells of interest (e.g., G_2 -M and tetraploid G_1).

BE is a premalignant condition associated with chronic gastroesophageal reflux in which the normal squamous epithelium is replaced by a metaplastic columnar epithelium. Patients with BE typically have symptoms of gastroesophageal reflux such as heartburn, and they frequently seek medical attention before they develop cancer. The Barrett's epithelium can be safely visualized and biopsied during upper gastrointestinal endoscopy, providing a highly favorable model for studying human neoplastic progression *in vivo* (13, 14). We have previously shown that diploid clones with $CDKN2A$ lesions are early prevalent lesions in BE capable of extensive clonal expansion (15–17). Furthermore, in the presence of somatically acquired $TP53$ lesions, these progenitors develop elevated 4N fractions, predisposing them to aneuploidy and to progressive clonal evolution that begins in premalignant cells, proceeds to cancer over a period of years, and continues after the emergence of cancer (5).

Primary cultures of Barrett epithelial cells [KR-42421 (CP-A), CP-52731 (CP-B), and CP-94251 (CP-C)] have been previously established from biopsies of patients with premalignant BE (18). Immortalized strains of primary cultures were derived by *hTERT* transduction to increase the number of replicate cultures and facilitate molecular studies of these cells. The Barrett epithelial cells contain $CDKN2A$ abnormalities (9pLOH, with mutation or promoter hypermethylation in the remaining allele, CP-A, CP-B, CP-C) and $TP53$ abnormalities (17p LOH and mutation in the remaining allele, CP-B, CP-C). All three cultures have elevated flow cytometric 4N (G_2 -tetraploid) DNA content fractions (CP-A 11.6%, CP-B 24.9%, and CP-C 22.8%) in the absence of aneuploidy. These same abnormalities were also present within the esophagi from which the cell strains were derived.

To investigate the molecular phenotype of these cell populations, we have used flow cytometry to enrich for tetraploid cells in the spontaneously arising 4N populations present in each of the BE cell cultures. The number of tetraploid cells in each sorted population was determined by FISH analysis with chromosome-specific centromeric probes. We used oligonucleotide arrays to identify genes that were differentially expressed in replicate 2N/4N comparisons in each cell strain and in *hTERT*-immortalized cultures of the $TP53^{mut}$ strains. This allowed a direct comparison of 4N cell populations of interest with isogenic diploid populations in the same experiment. In addition, to further characterize the cell cycle defects in these cells, we compared the expression profiles of sorted tetraploid cells to matching isogenic G_2 -sorted cells. Our analyses provide a detailed description of a key intermediate in neoplastic progression.

MATERIALS AND METHODS

Tissue Culture. Cell strains were established from BE biopsies and were maintained in modified MCDB 153 as described previously (18). The three parental strains used in this study were designated as KR-42421 (CP-A), CP-52731 (CP-B), and CP-94251 (CP-C). Two of the three cultures (CP-B and CP-C) were derived from biopsies taken from regions of high-grade dysplasia, whereas the third culture (CP-A) was initiated from biopsies taken from a region of nondysplastic metaplasia.

Received 11/26/02; accepted 5/7/03.

The costs of publication of this article were defrayed in part by the payment of page charges. This article must therefore be hereby marked *advertisement* in accordance with 18 U.S.C. Section 1734 solely to indicate this fact.

¹ Supported by NIH Grants PO1 CA91955, R01 CA78855, T32 AG00057 and R01 CA61202.

² Present address: Agilent Laboratories, 3500 Deer Creek Road, Palo Alto, CA 94304.

³ To whom requests for reprints should be addressed, at University of Washington, Department of Pathology, Box 357705, K081 Health Sciences Building, Seattle, WA 98195.

⁴ The abbreviations used are: BE, Barrett's esophagus; Rb, retinoblastoma; FISH, fluorescent *in situ* hybridization; RT-PCR, reverse transcription-PCR; LOH, loss of heterozygosity.

Flow Cytometry. Cells were incubated in growth media containing 10 μ M Hoechst 33342 (Calbiochem, La Jolla, CA) for 30 min at 37°C. Cells were subsequently trypsinized, resuspended in fresh media containing Hoechst dye, and kept at room temperature until sorting. All sorting was done using a Beckman-Coulter Elite cell sorter (Fullerton, CA).

RNA Extraction. All samples used for RNA preparations were fixed in RNAlater (Ambion, Austin TX) before extraction. Each sample was then homogenized by resuspension in lysis solution and passage through a Qiashredder (Qiagen, Valencia, CA) column. Total RNA was extracted with the Qiagen RNeasy Mini kit using the supplier's protocol.

cDNA Preparation. For each sample, double-stranded cDNA was prepared with GIBCO/BRL Superscript II (Invitrogen Life Technologies, Inc., Carlsbad, CA) using 5–10 μ g of total RNA as template. Subsequently, biotin-labeled cRNA was generated using the Enzo Bioarray RNA transcript-labeling kit (Affymetrix, Santa Clara, CA). All *in vitro* transcription reactions were carried out for 4–5 h according to the supplier's instructions. All RNA and cRNA samples were verified by ethidium bromide-stained gel analysis and quantified by SyBrII (Molecular Probes, Eugene, OR) fluorescence.

Array Hybridization and Data Analysis. All hybridizations were done with FL6800 chips (Affymetrix). A total of 25–50 μ g of each cRNA preparation was fragmented for 35 min at 94°C in buffer [40 mM Tris-acetate (pH 8.1)/100 mM magnesium acetate]. Aliquots of each cRNA preparation were then mixed with hybridization buffer at a final volume of 200 μ l. Each array was hybridized, washed, and scanned according to the manufacturer's instructions. Scanned output files for each independent experiment were analyzed by GeneChip MAS 5.0 software (Affymetrix) and exported into the database program Microsoft Access for additional analysis. The complete set of raw data files is available on line.⁵ Expression values for each experiment were derived from the Affymetrix absolute difference expression values. Genes differentially expressed between 2N and 4N cells were identified as follows: 2N/4N expression ratio and log₂-transformed expression ratios were first calculated. We then selected genes to analyze by using a filter to select genes consistently differentially expressed in both independent sets of a particular 2N to 4N comparison for both samples in 1 or more of the 10 experimental comparisons. Thus, the gene had to show a consistent increase [increase (I) or marginally increase (MI)] or decrease [decrease (D) or marginally decrease (MD)], using the Affymetrix MAS 5.0 differential expression calls, in both pairs of a sample (19). The differential expression call corresponded to *P* of differential expression of <0.003 as generated by the MAS 5.0 software (19). Because the replicate samples were truly independent (the cells for each pair of replicate were grown, processed, and hybridized at different times), the probability of consistent differential expression for one gene across both replicates of an experiment must be <0.00009. Because a gene was clustered if it was consistently up- or down-regulated in any 1 of the 10 replicate experiments, the expected number of observed differentially expressed genes under the null hypothesis that no genes were differentially expressed is $1 - (1 - 0.00009)^{10} \times (\text{analyzed experiments}) \times 2 \times 7129 \times (\text{number of genes on the array}) = 7.6$ genes. In our cluster analysis, we identified 625 genes that were consistently differentially expressed between 2N/4N samples in both replicate samples from one cell line comparison. Thus, we identified many more differentially expressed genes than the expected number of false positive genes under the null hypothesis.

The log₂-transformed expression ratios for these genes were subjected to pair wise average-linkage cluster analysis with the Cluster program (Michael Eisen)⁶ using Pearson's correlation as a distance metric. The log ratio used for clustering was the log ratio generated by MAS 5.0, except that in cases where MAS 5.0 called a no change (NC), the log₂ ratio was set to 0. The hierarchical tree was visualized using TreeView (M. Eisen).⁶ To identify genes differentially expressed in *TP53*^{wt} versus *TP53*^{mut} cells, clustering and data visualization followed the procedure used for the 2N/4N comparisons. All statistical tests used for this analysis were performed using Microsoft Excel.

FISH. Sorted cells were resuspended in 5 mM CaCl₂ then dropped onto clean slides and allowed to dry overnight. Slides were then processed for FISH as previously described using a rhodamine-labeled (red) chromosome 11 centromere probe (Vysis, Inc., Downers Grove, IL) and a FITC-labeled (green) chromosome 17 centromere probe (Vysis, Inc.) (20). Slides were counter-

stained with 0.23 μ g/ml 4', 6-diamidino-2-phenyl indole (Sigma), examined with \times 100 oil immersion on an epifluorescence microscope, and the numbers of red and green FISH spots were counted in each of at least 100 nuclei by a blinded observer. Cells were simultaneously evaluated for the presence of condensed mitotic chromatin. Cells were scored as tetraploid if they contained four or more red and four or more green spots. Because a FISH spot is sometimes overlapping or otherwise missed, cells with four red and three green or three red and four green spots were also counted as tetraploid.

Quantitative RT-PCR. Aliquots from total RNA samples used in the array experiments were used in real time PCR (TaqMan) assays. All assays were performed on the ABI Prism 7900 detection system (Applied Biosystems) using TaqMan EZ RT-PCR Core Reagents with glyceraldehyde-3-phosphate dehydrogenase controls for normalization. All reactions were done in triplicate according to the supplier's instructions. The primers and probes used in this study were: p55CDC20F, CATTACCCAGCATCAAGGG; p55CDC20 probe, CTGTCAAGCCGTAGCATGGTGTCC; p55CDC20R, CCAGGACATTGGACTGCCA; NEK2F, TGAGGACTATGAAGTGTGTACACCA; NEK2 probe, TGGCACAGGCTCTACGGCCG; NEK2R, CTCCGGATCTTCTGGCA; CENPAF, CCTTACATGCAGGCCGAGTT; CENPA probe, CTCTCTTCCAAAGGATGTGCAACTGG; CENPAR, CCCGGATCCTCCGG; RRM1F, CCTCAGAGCCTCAGCCACTAG; RRM1 probe, TGC-GATGCATGTGATCAAGCGAGA; and RRM1R, CTCGTTCTTGCGGCC.

RESULTS

To enrich for tetraploid cells in each 4N population, cells from asynchronous cultures were viably sorted into 2N (diploid G₁) and 4N (G₂-tetraploid) fractions (Fig. 1). The 2N cell fractions were stored, whereas the 4N cell fractions were recultured for 12–14 days to allow G₂ or transiently arrested cells to progress through the cell cycle and then re-sorted to obtain enriched 4N (tetraploid) cells. The expression profiles of single-sorted 2N and re-sorted 4N cell populations from each culture were compared in duplicate independent experiments. A total of 695 genes was identified that the GeneChip scoring software indicated were significantly differentially expressed (*P* < 0.003) in each of duplicate experiments comparing 2N versus 4N cells in each culture. Approximately 8 of these genes would be expected to be false positives (see "Materials and Methods"). Pairwise average linkage clustering identified a single predominant node of 124 genes (Fig. 2a).

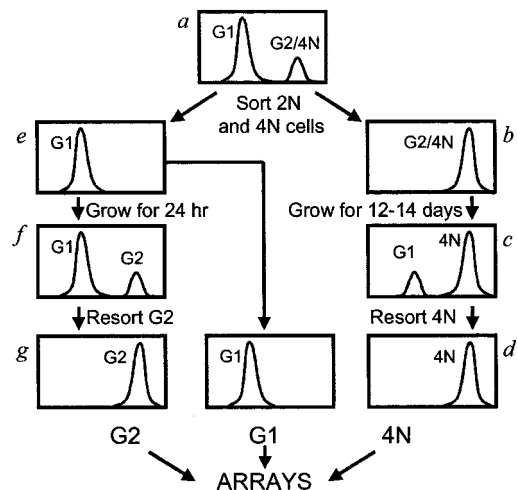


Fig. 1. Cell sorting enrichment of tetraploid and G₂ cells. *a*, asynchronous cultures containing 2N and 4N populations were sorted viably by DNA content (ploidy) using Hoechst 33242. The 2N cells (diploid G₁) from the first sort (*e*) were stored. The 4N cells (diploid G₂-tetraploid G₁) from the same sort (*b*) were returned to culture for 12–14 days to enrich for tetraploid-arrested cells (*c*). These were then resorted by ploidy to obtain enriched samples of 4N tetraploid cells (*d*). In separate experiments, populations of G₂ cells were obtained from 2N cells (diploid G₁) from the first sort (*e*) by returning these cells to culture for 24–48 h and resorting for G₂ cells (*g*). Samples *e* and *d* were processed in parallel for 2N/4N array analyses, whereas samples *e* and *g* were processed in parallel for 2N/G₂ array analyses.

⁵ Internet address: <http://www.fhcrc.org/phs/barretts/cancer-research/>.

⁶ Internet address: <http://www.microarrays.org/software>.

Fig. 2. Clustering and identification of genes differentially expressed in tetraploid Barrett's epithelial cells. Replicate experiments comparing flow sorted diploid and tetraploid populations were done with each of five cultures (CP-A, CP-B, CP-C, CP-B*hTERT*, and CP-C*hTERT*) with hierarchical clustering of the 695 differentially expressed genes (see text), illustrating (a) the cluster of 124 genes up-regulated in TP53 mutant 4N Barrett's epithelial cells. Expression of these same genes in G₂-G₁ comparisons is also illustrated (b).

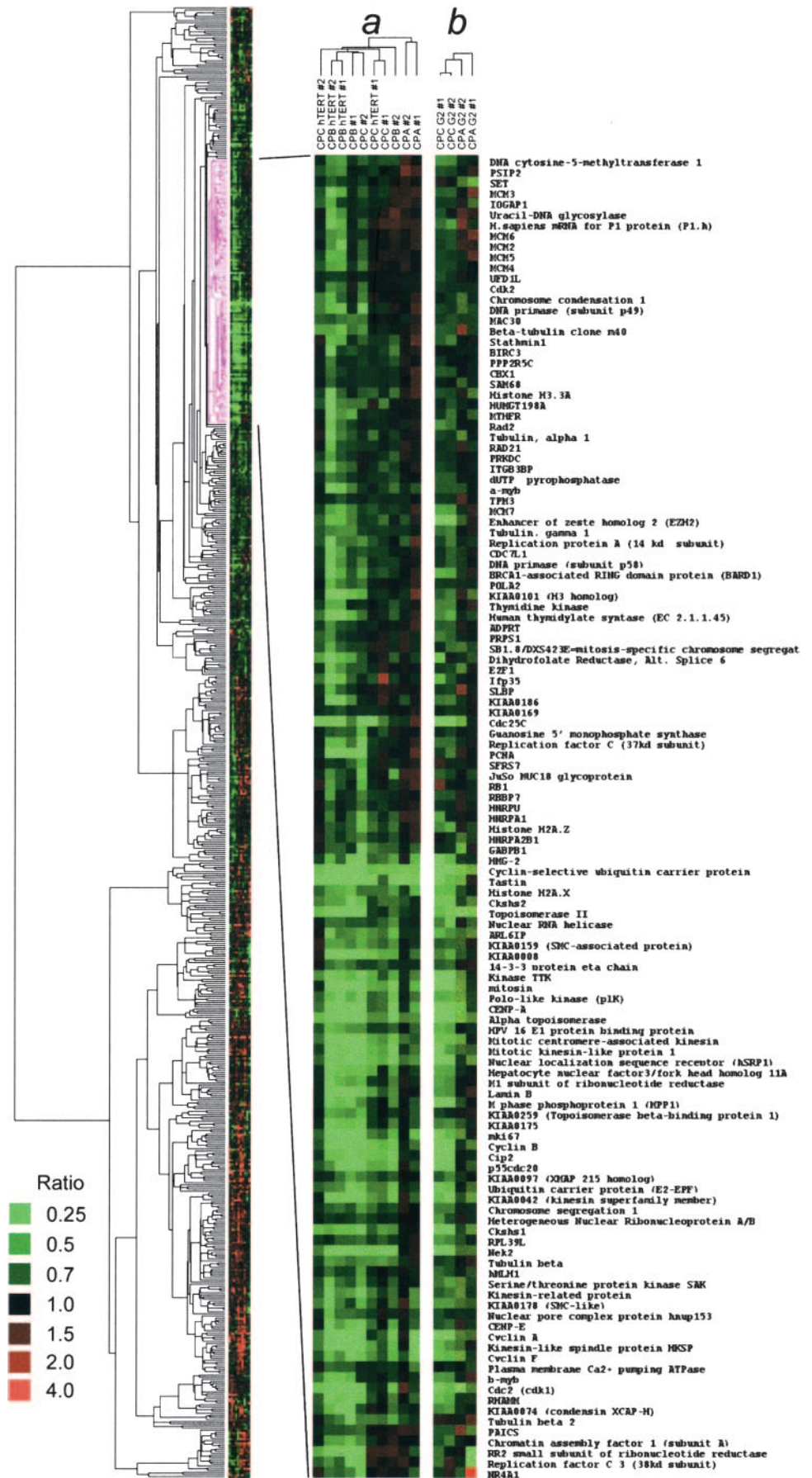


Table 1 Biological Function of Genes in TP53^{-/-} Tetraploid Cluster

Gene name	Accession number	Fold overexpression in 4N versus 2N cells ^a
DNA replication/repair (n = 18)		
<i>DNMT1</i> (DNA cytosine-5-methyltransferase 1)	X63692	1.7
<i>mK167</i>	X65550	5.4
<i>RPA3</i> (replication protein A 14 kd subunit)	L07493	2.0
<i>RRM1</i> (M1 subunit of ribonucleotide reductase)	X59543	2.3 ^b
<i>RRM2</i> (RR2 small subunit of ribonucleotide reductase)	X59618	1.9
<i>DHFR</i>	J00139	2.2
<i>RFC4</i> (replication factor C 37 kd subunit)	M87339	2.3
<i>RFC3</i> (replication factor C 38 kd subunit)	L07541	1.8
<i>POLA2</i> (DNA polymerase α -subunit p70)	L24559	1.5
<i>PRIM1</i> (DNA primase subunit p49)	X74330	2.0
<i>PRIM2A</i> (DNA primase subunit p58)	X74331	1.9
<i>TK1</i> (thymidine kinase)	M15205	1.6
<i>MTHFR</i>	J04031	1.9
<i>RAD21</i>	D38551	1.5
<i>PRKDC</i>	U47077	1.5
<i>DUT</i> (dUTP pyrophosphatase)	U31930	1.5
<i>Guanosine 5' monophosphate synthase</i>	HG4716-HT5158	1.5
<i>MLH1</i>	U07418	1.5
G ₁ -S transition (n = 8)		
<i>CDC7L1</i>	AB003698	1.8
<i>E2F1</i>	S49592	1.5
<i>PCNA</i>	M15796	3.0
<i>MCM3</i>	D38073	1.8
<i>MCM5</i>	X74795	1.5
<i>MCM4</i>	X74794	1.5
<i>MCM7</i>	D55716	1.9
<i>RB1</i>	L41870	1.5
G ₂ -M transition (n = 9)		
<i>CDK1</i>	X05360	5.7
<i>CCNB</i>	M25753	5.1
<i>CDC25C</i>	M34065	4.6
<i>CKS1</i> (CDC28 protein kinase 1)	X54941	3.2
<i>CKS2</i> (CDC28 protein kinase 2)	X54942	2.6
<i>CDKN3</i>	L25876	4.0
<i>CCNA</i>	X51688	3.8
<i>CCNF</i>	Z36714	3.2
<i>FOXM1</i> (hepatocyte nuclear factor3/forkhead homolog 11A)	U74612	5.4
Mitosis (n = 42)		
Chromosome segregation (n = 22)		
<i>CENPF</i> (mitosin)	U30872	5.0
<i>HKSP</i> (kinesin-like spindle protein)	U37426	5.1
<i>KNSL1</i> (kinesin-related protein)	X85137	2.8
<i>KNSL6</i> (mitotic centromere-associated kinesin)	U63743	4.3
<i>KNSL5</i> (mitotic kinesin-like protein 1)	X67155	5.2
<i>CENPE</i>	Z15005	3.0
<i>KIAA0042</i> (kinesin superfamily member)	D26361	4.2
<i>SMC1L1</i>	D80000	2.2
<i>KIAA0159</i> (SMC-associated protein)	D63880	2.1
<i>TOP2A</i> (topoisomerase II α)	J04088	4.7
α Topoisomerase (truncated form)	L47276	7.0
<i>TOPBP1</i> (topoisomerase β -binding protein 1)	D87448	1.9
<i>p55CDC20</i>	U05340	3.8 ^b
<i>TTK</i>	M86699	3.5
<i>PLK</i> (polo-like kinase)	U01038	3.0
<i>STK18</i>	Y13115	1.9
<i>E2-EPF</i> (ubiquitin carrier protein)	M91670	2.8
<i>NEK2</i>	Z29066	6.8 ^b
<i>UBE2C</i> (cyclin-selective ubiquitin carrier protein)	U73379	7.6
<i>MPP1</i> (M-phase phosphoprotein 1)	L16782	2.4
<i>CSE1L</i> (chromosome segregation 1)	U33286	1.8
<i>STMN1</i> (stathmin 1)	M31303	1.5
Chromatin organization (n = 20)		
<i>CENP-A</i>	U14518	5.0 ^b
<i>HMG-2</i>	X62534	2.9
<i>LMNB</i>	M34458	3.7
KIAA0101 (H3 homologue)	D14657	2.5
KIAA0074 (condensin <i>XCAPH</i>)	D38553	2.4
<i>TUBB1</i> (β -Tubulin clone m40)	J00314	1.9
Tubulin β	HG4322-HT4592	1.5
Tubulin β 2	HG1980-HT2023	2.3
KIAA0097 (<i>XMAP</i> 215 homologue)	D43948	1.8
<i>EZH2</i> (Enhancer of zeste homologue 2)	U61145	2.0
<i>H2A.X</i>	X14850	2.4
<i>CHC1</i> (chromosome condensation 1)	D00591	1.5
<i>H3.3A</i>	X05855	1.8
<i>TUBA1</i>	X06956	1.7

Table 1 Continued

Gene name	Accession number	Fold overexpression in 4N versus 2N cells ^a
<i>TUBG1</i>	M61764	1.8
<i>RBBP7</i>	X72841	1.5
<i>HNRPA1</i>	U00947	1.7
<i>H2A.Z</i>	M37583	1.8
<i>HNRPA2B1</i>	M29064	1.5
<i>CHAF1A</i> (chromatin assembly factor 1 subunit A)	U20979	1.7
Cell adhesion (n = 4)		
<i>TROAP</i> (Tastin)	U04810	7.7
<i>RHAMM</i>	U29343	3.7
<i>MCAM</i> (JuSo MUC18 glycoprotein)	M28882	1.7
<i>ITGB3BP</i>	U37139	1.8
Other (n = 14)		
<i>YWAH</i> (14-3-3 protein ζ chain)	D78577	1.6
<i>BIRC3</i>	U37547	1.7
<i>BARD1</i> (BRCA1-associated RING domain protein)	U76638	2.0
<i>DDXL</i> (nuclear RNA helicase)	U90426	2.0
<i>KPNA2</i> (nuclear localization sequence receptor)	U28386	5.4
<i>NUP153</i> (nuclear pore complex protein hnp153)	Z25535	1.7
<i>a-MYB</i>	X66087	2.1
<i>b-MYB</i>	X13293	2.0
<i>PSIP2</i>	U94319	1.5
<i>HUMGT198A</i>	L38933	1.9
<i>GABPB1</i>	HG1686-HT4572	2.2
<i>ARL6IP</i>	D31885	2.4
<i>RPL39L</i>	HG2874-HT3018	1.7
<i>NR4A1</i>	L13740	1.5
Unknown function (n = 6)		
<i>MAC30</i>	L19183	1.5
HPV 16 E1 protein-binding protein	U96131	2.1
Ipf35	L78833	1.9
KIAA0008	D13633	4.3
KIAA0175	D79997	2.5
KIAA0186	D80008	1.8

^a Average values from duplicate experiments with each TP53^{-/-} cells (CP-B, CP-C, CP-BhTERT, and CP-ChTERT).

^b Fold increases confirmed by real-time PCR assays as shown in supplemental Fig. 1 available on line.⁵

Strikingly, all of these genes were uniquely overexpressed in the 4N TP53^{mut} cultures and of those showing ≥ 1.5 -fold changes (101 of 124), most have G₂-M-related functions (Table 1). These genes are hereafter referred to as the TP53^{mut} gene cluster.

Examples of these genes include *CDK1* and regulators of CDK1 activation (*CDC25C*, *CCNB*, *CCNA*, *CCNF*, *CKS1*, *CKS2*, and *CDKN3*) that control progression through G₂ and entry into mitosis (21, 22). The largest functional group consists of mitosis-associated genes. These include mediators of chromosome segregation such as the centrosomal kinase *NEK2*, regulators of the anaphase-promoting complex (*p55CDC20*, *PLK*, *CSE1L*, and *E2-EPF*), microtubule-dependent motor proteins (*CENPF*, *CENPE*, and *HKSP*), and cohesin (*SMC*) subunits (23–27). The node also contained genes associated with chromatin structure and condensation (*CENPA*, core histones, *XCAPH*, and *EZH2*), cell adhesion (*RHAMM*, *TROAP*, and *MCAM*), and 7 genes of unknown function that may also mediate some of these processes. The striking functional conservation of these genes additionally validates our clustering results. The altered expression of 4 of the genes in the node, *RRM1*, *p55CDC2*, *CENP-A*, and *NEK2* was confirmed by real-time RT-PCR (supplemental Fig. 1 available on line),⁵ although the absolute magnitude of expression differences was larger by RT-PCR, as has been found by many other investigators.

Although these genes included some of the major regulators of the G₂-M phase of the cell cycle, we did not detect mitotic chromosomes in the nuclei of the re-sorted 4N cell populations. FISH analysis with chromosome 11 and 17-specific centromeric probes revealed variable numbers of tetraploid cells (23.5–81.5%) in each of the re-sorted 4N

Table 2. FISH analysis of flow-sorted cells

Cell culture	% tetraploid cells		4N/2N expression ratio ^a
	2N Sort	4N Sort	
CP-A	2.5	73	1.1
CP-B	0	23.5	2.2
CP-C	0	75	2.0
CP-BhTERT	0	35	3.3
CP-ChTERT	1	81.5	1.5

^a Average 4N/2N gene expression ratio of the entire 124 gene cluster shown in Fig. 2a and Table 1.

cell populations (Table 2). However, the mean expression level of the 124 gene 4N *TP53*^{mut} cluster was not significantly related to the percentage of tetraploid cells in the sorted 4N fractions by regression analysis and was similar in *TP53*^{mut} cells with low (CP-B, CP-BhTERT) or high (CP-C, CP-ChTERT) proportions of tetraploid cells (paired *t* test).

In comparison, 4N *TP53*^{wt} cells (CP-A), although mainly (73%) tetraploid by FISH analysis, displayed little difference in expression pattern with their isogenic 2N cells (2.5% tetraploid) in the filtered set of 695 genes (Fig. 2a). Therefore, we reanalyzed the absolute expression values for all 20 hybridizations in the 2N versus re-sorted 4N cell populations dataset and looked for differences between *TP53*^{wt} and *TP53*^{mut} strains. This identified a unique set of 42 genes that was up-regulated in both 2N and 4N *TP53*^{wt} cells compared with the *TP53*^{mut} cell populations and included *TP53*-regulated inhibitors of G₁-S and G₂-M such as *CDKN1A* and *SFN* (supplemental Figs. 2, A and B, available on line).⁵

G₂ Cell Populations. To additionally characterize the molecular phenotype of the 4N cell populations, we used flow cytometry to obtain enriched populations of G₂ cells from *TP53*^{wt} strain (CP-A) and a *TP53*^{mut} population (CP-ChTERT) with high tetraploid cell content (81.5%) in the 4N fraction. 2N (diploid G₁) cells from asynchronous cultures were viably sorted and then returned to culture for 24–48 h to allow cells to transit through the cell cycle into G₂; the G₂ cells were then purified by re-sorting according to DNA content (Fig. 1). The time points used between 24 and 48 h were selected based on the reappearance of G₂ cells in the culture and the absence of tetraploid cells as determined in FISH analyses (data not shown). There were 452 genes overexpressed in one or more G₂ cell culture, and 135 that were underexpressed (supplemental Fig. 3 available on line).⁵ The expression profiles of *TP53*^{mut} G₂ populations were similar to the re-sorted 4N *TP53*^{mut} cells. In contrast, the expression profile of *TP53*^{wt} G₂ cells was distinct from isogenic re-sorted 4N and 2N cells but was similar to that of the *TP53*^{mut} G₂ populations and included the up-regulation of many of the cell cycle-specific genes in the 4N *TP53*^{mut} cluster.

DISCUSSION

Previous studies using flow cytometry and genotyping have validated the role of elevated 4N fractions (>6%) in diploid biopsies as a key transition in the development of aneuploidy and the subsequent progression to cancer (3, 5–7). However, the genetic and cellular heterogeneity of solid tumors makes it difficult to comprehensively study this key intermediate of neoplastic progression. Several reports using tumor cell line model systems have shown that elevated 4N fractions are associated with lesions in the cell cycle and disruption of G₂-M. However, investigating G₂-M cell populations in these studies typically relies on the synchronization of immortalized cells, which is frequently imperfect (22, 28, 29).

The cell cultures in this study were derived from endoscopic

biopsies obtained from patients with premalignant BE in the absence of cancer. Each of the strains has a finite life span and contains genetic lesions associated with early stages of neoplastic progression *in vivo*, including inactivation of *CDKN2A* and *TP53* (18). These same lesions were present in the biopsies from which they were derived. Furthermore, each of the strains and the hTERT-immortalized cultures of the *TP53*^{mut} strains contain spontaneously arising 4N cell fractions in the absence of aneuploidy. Therefore, our combination of flow cytometry, FISH, and oligonucleotide array expression analysis provides the first genome-wide analysis of spontaneously arising tetraploid cells in a premalignant tissue.

DNA content flow cytometry can purify cells from different stages of the cell cycle without the need for synchronization. However, it cannot distinguish between tetraploid G₁ cells and diploid G₂ cells in a mixed 4N cell population. Therefore, we used FISH analysis with chromosome 11 and 17-specific centromeric probes to quantify the tetraploid (four spots/probe) and G₂ (two spots/probe) cell content in each of the re-sorted 4N populations (Table 2). There was a wide variation in the tetraploid content present in the re-sorted 4N cell populations. However, the mean expression level of the 124 gene 4N *TP53*^{mut} cluster was similar in *TP53*^{mut} cells with low (CP-B, 23.5% and CP-BhTERT, 35%) or high (CP-C, 75% and CP-ChTERT, 81.5%) proportions of tetraploid cells (paired *t* test).

Previous studies using synchronized normal human fibroblast cell cultures and the same oligonucleotide array platform identified 387 genes with periodic expression during distinct phases of the cell cycle (30). These included 47 of 124 genes that we observe in the 4N *TP53*^{mut} cluster. Most of these 47 cell cycle-regulated transcripts in the 4N *TP53*^{mut} cluster (36 of 47: 77%) are up-regulated during normal entry and transition through mitosis. These include mediators of G₂-M transition (*CDK1*, *CCNB*, and *CCNA*) and the major events of mitosis such as chromosome condensation (*TOP2A* and *CHC1*), centrosome separation and activation (*NEK2* and *PLK*), spindle assembly (*HKSP*, *KNSL5*, and *KNSL6*), and chromosome segregation (*p55CDC20*, *CENPF*, *CENPE*, and *UBE2C*; Refs. 25–27, 31–33).

The order of events in cell cycle is essential for genomic stability and is ensured by checkpoint dependency. For example, segregation of chromosomes during mitosis relies on the proper regulation of chromosomal DNA replication and centrosome duplication in the preceding S phase (32, 34). Furthermore, both of these processes are dependent on the phosphorylation of the *Rb* gene product and subsequent levels of free *E2F* gene family members (34–36). The largest functional category present in the 4N *TP53*^{mut} cluster contained regulators of progression through G₂ and entry into mitosis. These included a series of kinases, including *CDK1*, *PLK1*, *NEK2*, and *TTK*, that regulate cell division and associated checkpoints (31). In addition, the cluster also contained activators (*CCNB*, *CDC25C*, and *p55CDC20*) and targets (*LMNB1* and *CENPA*) of these cell cycle-regulatory kinases. The up-regulation of these genes and the overabundance of transcripts with a mitosis-specific temporal pattern among the cell cycle-regulated genes suggest that 4N *TP53*^{mut} BE cells are activating a mitotic transcriptional program. However, despite these expression patterns, there was an absence of mitotic cells in these populations.

The cells and the biopsies from which they were derived contain regions of LOH, and this reflects DNA damage during neoplastic progression (18). In addition, *CDKN2A* abnormalities (9pLOH, with mutation or promoter hypermethylation in the remaining allele) were present in each culture. The cells with methylated alleles did not express any *CDKN2A* transcript as determined in our array studies, whereas the mutated allele encodes a missense mutation that is known to inhibit normal function of *CDKN2A* (37). Several of the genes in

the 4N *TP53*^{mut} cluster, including regulators of G₂-M (*PLK*, *TTK*, *CENPE*, *NEK2*, *CDK1*, and *TOPO2A*), are transcriptionally repressed by *E2F4* binding and its interactions with Rb pocket proteins and histone deacetylases in noncycling cells (36, 38). Furthermore, several genes in the 4N *TP53*^{mut} cluster (e.g., *CKS1*, *SMC*, *TOP2A*, *YWHAH*, and *BARD1*) are activated in response to DNA damage and mediate various cell cycle checkpoints (39).

Studies with immortalized tumor cells have shown that in the presence of drug-induced double-strand DNA breaks cycling cells may activate a reversible G₂ arrest (28). This arrest is associated with a prolonged induction of G₂-M-associated genes. In addition to enriching for spontaneously arising tetraploid populations, we used flow cytometry to obtain G₂ cell fractions without the need for extensive synchronization. Within the 4N *TP53*^{mut} cluster, the expression profile of the 4N *TP53*^{mut} populations (Fig. 2b) was similar to the G₂ *TP53*^{wt} cells, suggesting that the former phenotype arose from a G₂ delay. The *CDKN2A*-null background of BE cells likely disrupts *CDK4* regulation, creating a condition permissive for *TP53*^{mut} cells with genomic lesions to transit through G₁-S, overcome *E2F4* repression and activate a G₂-M transcriptional program. Consequently, 4N *TP53*^{mut} cells either delay in early G₂-M (CP-B, CP-B*hTERT*) with low tetraploid fractions or transit from G₂-M to the tetraploid G₁ by adaptation (CP-C, CP-C*hTERT*) in the absence of condensed chromosomes (40–42).

The 4N *TP53*^{wt} cells, although primarily tetraploid (73%), retain the expression profile of the diploid cells from which they arose (Fig. 2, Table 2). Furthermore, both of these *TP53*^{wt} cell populations were distinct from the isogenic G₂ populations. Previous *in vitro* studies have shown that disruption of the mitotic spindle results in the activation of a tetraploid G₁ checkpoint in diploid human cells (11). Activation of this checkpoint is dependent on exit from mitosis, reentry into G₁, and *TP53*-induced *CDKN1A* expression. The 42 gene *TP53*^{wt} set included *CDKN1A* and was present in both diploid and tetraploid cell populations, suggesting that this checkpoint was activated. Furthermore, the absence of *CDKN1A* in *TP53*^{wt} G₂ cells is consistent with the G₁-specific activation of the tetraploid checkpoint. In contrast, the *TP53*^{mut} 4N cells enter G₂ inappropriately and subsequently activate a G₂-M transcriptional program, which can persist even if the cells progress to a tetraploid G₁ by accommodation. The *TP53*^{mut} 4N cluster identifies pathways that contribute to mitotic and chromosomal instability, perhaps accounting for the increased cancer risk associated with the presence of elevated 4N fractions in BE.

ACKNOWLEDGMENTS

We thank Jeff Delrow, Cassie Neal, Ryan Bosom, and Dan Hare for assistance with microarray experiments.

REFERENCES

- Shackney, S. E., Smith, C. A., Miller, B. W., Burholt, D. R., Murtha, K., Giles, H. R., Ketterer, D. M., and Pollice, A. A. Model for the genetic evolution of human solid tumors. *Cancer Res.*, *49*: 3344–3354, 1989.
- Hollstein, M., Sidransky, D., Vogelstein, B., and Harris, C. C. p53 mutations in human cancers. *Science (Wash. DC)*, *253*: 49–53, 1991.
- Galipeau, P. C., Cowan, D. S., Sanchez, C. A., Barrett, M. T., Emond, M. J., Levine, D. S., Rabinovitch, P. S., and Reid, B. J. 17p (p53) allelic losses, 4N (G₂/tetraploid) populations, and progression to aneuploidy in Barrett's esophagus. *Proc. Natl. Acad. Sci. USA*, *93*: 7081–7084, 1996.
- Blount, P. L., Galipeau, P. C., Sanchez, C. A., Neshat, K., Levine, D. S., Yin, Y., Suzuki, H., Abraham, J. M., Meltzer, S. J., and Reid, B. J. 17p allelic losses in diploid cells of patients with Barrett's esophagus who develop aneuploidy. *Cancer Res.*, *54*: 2292–2295, 1994.
- Barrett, M. T., Sanchez, C. A., Prevo, L. J., Wong, D. J., Galipeau, P. C., Paulson, T. G., Rabinovitch, P. S., and Reid, B. J. Evolution of neoplastic cell lineages in Barrett oesophagus. *Nat. Genet.*, *22*: 106–109, 1999.
- Rabinovitch, P. S., Longton, G., Blount, P. L., Levine, D. S., and Reid, B. J. Predictors of progression in Barrett's esophagus III: baseline flow cytometric variables. *Am. J. Gastroenterol.*, *96*: 3071–3083, 2001.
- Reid, B. J., Levine, D. S., Longton, G., Blount, P. L., and Rabinovitch, P. S. Predictors of progression to cancer in Barrett's esophagus: baseline histology and flow cytometry identify low- and high-risk patient subsets. *Am. J. Gastroenterol.*, *95*: 1669–1676, 2000.
- Cross, S. M., Sanchez, C. A., Morgan, C. A., Schimke, M. K., Ramel, S., Idzerda, R. L., Raskind, W. H., and Reid, B. J. A p53-dependent mouse spindle checkpoint. *Science (Wash. DC)*, *267*: 1353–1356, 1995.
- Fukasawa, K., Choi, T., Kuriyama, R., Rulong, S., and Vande Woude, G. F. Abnormal centrosome amplification in the absence of p53. *Science (Wash. DC)*, *271*: 1744–1747, 1996.
- DiLeonardo, A., Khan, S. H., Linke, S. P., Greco, V., Seidita, G., and Wahl, G. M. DNA replication in the presence of mitotic spindle inhibitors in human and mouse fibroblasts lacking either p53 or pRb function. *Cancer Res.*, *57*: 1013–1019, 1997.
- Khan, S. H., and Wahl, G. M. p53 and pRb prevent rereplication in response to microtubule inhibitors by mediating a reversible G₁ arrest. *Cancer Res.*, *58*: 396–401, 1998.
- Andreassen, P. R., Lohez, O. D., Lacroix, F. B., and Margolis, R. L. Tetraploid state induces p53-dependent arrest of nontransformed mammalian cells in G₁. *Mol. Biol. Cell*, *12*: 1315–1328, 2001.
- Neshat, K., Sanchez, C. A., Galipeau, P. C., Cowan, D. S., Ramel, S., Levine, D. S., and Reid, B. J. Barrett's esophagus: A model of human neoplastic progression. *Cold Spring Harbor Symp. on Quant. Biol.*, *59*: 577–583, 1994.
- Levine, D. S., Blount, P. L., Rudolph, R. E., and Reid, B. J. Safety of a systematic endoscopic biopsy protocol in patients with Barrett's esophagus. *Am. J. Gastroenterol.*, *95*: 1152–1157, 2000.
- Wong, D. J., Paulson, T. G., Prevo, L. J., Galipeau, P. C., Longton, G., Blount, P. L., and Reid, B. J. p16(INK4a) lesions are common, early abnormalities that undergo clonal expansion in Barrett's metaplastic epithelium. *Cancer Res.*, *61*: 8284–8289, 2001.
- Prevo, L. J., Sanchez, C. A., Galipeau, P. C., and Reid, B. J. p53-mutant clones and field effects in Barrett's esophagus. *Cancer Res.*, *59*: 4784–4787, 1999.
- Galipeau, P. C., Prevo, L. J., Sanchez, C. A., Longton, G. M., and Reid, B. J. Clonal expansion and loss of heterozygosity at chromosomes 9p and 17p in premalignant esophageal (Barrett's) tissue. *J. Natl. Cancer Inst. (Bethesda)*, *91*: 2087–2095, 1999.
- Palanca-Wessels, M. C., Barrett, M. T., Galipeau, P. C., Rohrer, K. L., Reid, B. J., and Rabinovitch, P. S. Genetic analysis of long-term Barrett's esophagus epithelial cultures exhibiting cytogenetic and ploidy abnormalities. *Gastroenterology*, *114*: 295–304, 1998.
- Liu, W. M., Mei, R., Bartell, D. M., Di, X., Webster, T. A., and Ryder, T. Rank-based algorithms for analysis of microarrays. *Proc. SPIE*, *4266*: 56–67, 2001.
- Rabinovitch, P. S., Dziadon, S., Brentnall, T. A., Emond, M. J., Crispin, D. A., Haggitt, R. C., and Bronner, M. P. Pancolonic chromosomal instability precedes dysplasia and cancer in ulcerative colitis. *Cancer Res.*, *59*: 5148–5153, 1999.
- Pines, J., and Rieder, C. L. Re-staging mitosis: a contemporary view of mitotic progression. *Nat. Cell Biol.*, *3*: E3–E6, 2001.
- Taylor, W. R., and Stark, G. R. Regulation of the G₂-M transition by p53. *Oncogene*, *20*: 1803–1815, 2001.
- Karsenti, E., and Vernos, I. Cell cycle—the mitotic spindle: a self-made machine. *Science (Wash. DC)*, *294*: 543–547, 2001.
- Nasmyth, K., Peters, J. M., and Uhlmann, F. Splitting the chromosome: cutting the ties that bind sister chromatids. *Science (Wash. DC)*, *288*: 1379–1384, 2000.
- Zachariae, W., and Nasmyth, K. Whose end is destruction: cell division and the anaphase-promoting complex. *Genes Dev.*, *13*: 2039–2058, 1999.
- Page, A. M., and Hieter, P. The anaphase-promoting complex: new subunits and regulators. *Annu. Rev. Biochem.*, *68*: 583–609, 1999.
- Morgan, D. O. Regulation of the APC and the exit from mitosis. *Nat. Cell Biol.*, *1*: E47–E53, 1999.
- Zhou, Y., Gwadry, F. G., Reinhold, W. C., Miller, L. D., Smith, L. H., Scherf, U., Liu, E. T., Kohn, K. W., Pommier, Y., and Weinstein, J. N. Transcriptional regulation of mitotic genes by camptothecin-induced DNA damage: microarray analysis of dose- and time-dependent effects. *Cancer Res.*, *62*: 1688–1695, 2002.
- Andreassen, P. R., Lacroix, F. B., Lohez, O. D., and Margolis, R. L. Neither p21^{WAF1} nor 14-3-3 prevents G₂ progression to mitotic catastrophe in human colon carcinoma cells after DNA damage, but p21^{WAF1} induces stable G₁ arrest in resulting tetraploid cells. *Cancer Res.*, *61*: 7660–7668, 2001.
- Cho, R. J., Huang, M. X., Campbell, M. J., Dong, H. L., Steinmetz, L., Sapinoso, L., Hampton, G., Elledge, S. J., Davis, R. W., and Lockhart, D. J. Transcriptional regulation and function during the human cell cycle. *Nat. Genet.*, *27*: 48–54, 2001.
- Nigg, E. A. Mitotic kinases as regulators of cell division and its checkpoints. *Nat. Rev. Mol. Cell Biol.*, *2*: 21–32, 2001.
- Hinchcliffe, E. H., and Sluder, G. "It takes two to tango": understanding how centrosome duplication is regulated throughout the cell cycle. *Genes Dev.*, *15*: 1167–1181, 2001.
- Glover, D. M., Hagan, I. M., and Tavares, A. A. M. Polo-like kinases: a team that plays throughout mitosis. *Genes Dev.*, *12*: 3777–3787, 1998.
- Meraldi, P., Lukas, J., Fry, A. M., Bartek, J., and Nigg, E. A. Centrosome duplication in mammalian somatic cells requires E2F and Cdk2-cyclin A. *Nat. Cell Biol.*, *1*: 88–93, 1999.

35. Lukas, C., Sorensen, C. S., Kramer, E., Santoni-Rugiu, E., Lindeneg, C., Peters, J. M., Bartek, J., and Lukas, J. Accumulation of cyclin B1 requires E2F and cyclin-A-dependent rearrangement of the anaphase-promoting complex. *Nature (Lond.)*, *401*: 815–818, 1999.
36. Ren, B., Cam, H., Takahashi, Y., Volkert, T., Terragni, J., Young, R. A., and Dynlacht, B. D. E2F integrates cell cycle progression with DNA repair, replication, and G₂-M checkpoints. *Genes Dev.*, *16*: 245–256, 2002.
37. Ranade, K., Hussussian, C. J., Sikorski, R. S., Varmus, H. E., Goldstein, A. M., Tucker, M. A., Serrano, M., Hannon, G. J., Beach, D., and Dracopoli, N. C. Mutations associated with familial melanoma impair p16INK4 function. *Nat. Genet.*, *10*: 114–116, 1995.
38. Rayman, J. B., Takahashi, Y., Indjeian, V. B., Dannenberg, J. H., Catchpole, S., Watson, R. J., Riele, H., and Dynlacht, B. D. E2F mediates cell cycle-dependent transcriptional repression *in vivo* by recruitment of an HDAC1/mSin3B corepressor complex. *Genes Dev.*, *16*: 933–947, 2002.
39. Zhou, B. B. S., and Elledge, S. J. The DNA damage response: putting checkpoints in perspective. *Nature (Lond.)*, *408*: 433–439, 2000.
40. Pellicioli, A., Lee, S. B., Lucca, C., Foiani, M., and Haber, J. E. Regulation of *Saccharomyces* Rad53 checkpoint kinase during adaptation from DNA damage-induced G₂-M arrest. *Mol. Cell*, *7*: 293–300, 2001.
41. Paulovich, A. G., Toczyski, D. P., and Hartwell, L. H. When checkpoints fail. *Cell*, *88*: 315–321, 1997.
42. Galgoczy, D. J., and Toczyski, D. P. Checkpoint adaptation precedes spontaneous and damage-induced genomic instability in yeast. *Mol. Cell. Biol.*, *21*: 1710–1718, 2001.